www.cafetinnova.org

Indexed in
Scopus Compendex and Geobase Elsevier,
Geo-Ref Information Services-USA, List B of Scientific
Journals, Poland, Directory of Research Journals

ISSN 0974-5904, Volume 09, No. 02

International Journal of Earth Sciences and Engineering

April 2016, P.P.731-737

Prospecting Potential and Accumulation Conditions of Shale Gas in the North of Ordos Basin, North China: Taking the Taiyuan and Shanxi Formations as Examples

HAIPENG YAO[1,2] AND YANMING ZHU[1]
[1]*School of Resource and Geosciences, CUMT, Xuzhou, Jiangsu 221008, China*
[2]*Coal Geological Bureau of the Inner Mongolia Autonomous Region, Hohhot 010010, China*
Email: *yaohp_cumt@sina.com*

Abstract: The Taiyuan and Shanxi formations have great shale gas exploration potential in the northern Ordos Basin. With the geological and geochemical analysis, the shale of Shanxi and Taiyuan formations were studied with the sedimentary facies characteristics, TOC, organic carbon type and maturity. With the NMR logging and field desorption experiment, the reservoir characteristics and shale gas concentration were analyzed in the two formations. The results showed that the shale is well developed thickly and distributed in the two sections of Taiyuan formation and the upper two sections of Shanxi formation. The siltstone or sandstone sandwiched with the mudstone has favorite reservoir space for shale gas. The shale has high content of humic organic matter, which now benefits for generating gas at the maturity stage and over-mature stage. The Taiyuan mudstone is brittle with more quartz, while the Shanxi mudstone has more clay content with micro pores. The clay mineral of two formations primarily consists of the kaolinite and illite. The reservoir space includes the matrix pores and fractures decided by the development degree of pores and fractures. The Taiyuan formation has higher gas content than Shanxi formation including the shale and the sandstone, especially higher gas content in the coal.

Keywords: *Shale gas; accumulation conditions; Shanxi and Taiyuan formations; Ordos Basin*

1. Introduction

In recent years, the global exploration activities of shale gas make a far-reaching impact on the exploration and development of unconventional natural gas, especially successful commercial exploitation in the United States and Canada [1~4]. Many countries are increasing the shale gas research and resource evaluation, and make significant progress, such as Alum shale in Sweden, Silurian shale in Poland, Neuquen shale in Argentina, and Mikulov shale in Austria [5~9]. In China, the shale gas exploration is active in the Sichuan Basin, Ordos Basin, Bohai Bay Basin, Songliao Basin, Tuha Basin, Jianghan Basin, Junggar Basin and Tarim Basin. The basins develop the marine, paralic, and continental facies shale with good hydrocarbon accumulation geological conditions [10~14]. Based on the Chinese resources estimates from Zhao et al. (2012)[15], the exploitation resource amount of shale gas is about 10,000 billion cubic meters, which counts half of conventional natural gas resource.

Ordos Basin has the advantages of unconventional gas reservoir geological conditions and rich resources, regarding as a research focus of unconventional gas in China [16~19]. In this basin, the mudstone and coal are mainly distributed in the Taiyuan and Shanxi formations of the Upper Paleozoic, which extend relatively stable with a little thickness in both of the eastern and western basin. The formations have high abundance of organic matter with high thermal evolution degree, and have strong gas generation ability [20-23]. In this study, the Taiyuan and Shanxi formations in the northern Ordos Basin were selected for the shale gas enrichment geological conditions, which provide the relevant parameters for the next shale gas exploration.

2. Geological Setting

The Ordos Basin has an area of 37×10^4 km^2 as the second biggest sedimentary basin in China. In this work, the northern basin was studied and divided into four parts (Figure 1), which are Yimengbei uplift, Yishan slope, Central uplift, and Tianhuan sag. The Tianhuan sag shows a synclinal structure with a gentle eastern limb and steep western one, which formed during the Cretaceous. The Central uplift occurred in a palaeohigh during the late Carboniferous to early Permian. The Yishan slope is gentle with small nosing structure. The Yimengbei uplift is a long-term inherited palaeohigh with the WE striking, and the lower Palaeozoic and bottom of upper Palaeozoic are missing. The slope and uplifts generally show a structural property of higher in the north and east. The EY-1 well is a first exploratory test well of shale gas in this area.

The basin base is composed of metamorphic rock from the Archean Erathem and lower Proterozoic. From bottom to top, the sedimentary strata are the Cambrian, Ordovician, Carboniferous, Permian, Triassic, Jurassic, Cretaceous, and Cenozoic. The

lower Palaeozoic mainly deposited the marine carbonate rocks, while it occurred in the continental sedimentation of fluvial and lake facies for the upper Palaeozoic and Cenozoic, such as the gravel, sandstone, mudstone, and coal. In the study area, the Lower Carboniferous is lost, and the Taiyuan formation (C_2t) develops as the Upper Carboniferous, which is less than 96 m thick and composed of sandstone, aluminous mudstone, battie, carbonate rock. However the Permian develops well, and is divided into four formations from top to bottom, which are Sunjiagou (P_3s), Shangshihezi (P_2s), Xiashihezi (P_2x), and Shanxi (P_1s) formations. The Shanxi formation is less than 140 m, and consists of the mudstone, siltstone, fine sandstone, pebbled sandstone, and coal with some phytolite. In Ordos Basin, the dark shale of Palaeozoic develops in the Taiyuan formation of Upper Carboniferous and Shanxi formation of Lower Permian, which are both potential gas-generation strata.

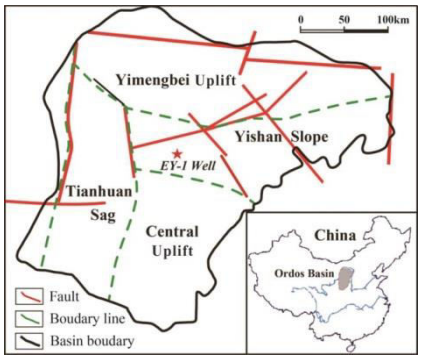

Figure1. *Location and regional structure of the north of Ordos Basin, North China*

3. Sample and Methods

By the geochemical and logging analysis of the drilling core and cuttings, the source rock and reservoir were evaluated in the study area. The TOC content was tested with the Carbon-Sulfur Analyzer of CS-230 Type in the China University of Mining and Technology. At the same time, the maceral was distinguished in the microscope, and so did the organic matter type and vitrinite reflectance. The whole rock mineral analysis of shale was analyzed with the X-ray diffraction Analyzer of YST-I Type, and then used to decide the clay mineral type. The pores of shale were observed by the scanning electron microscope (SEM). In addition, the porosity and permeability of shale were obtained with the nuclear magnetic logging (NML) and mercury intrusion method of the drilling core. For the EY-1 well, the data of gas bearing capacity were obtained with the shale field desorption analyzer, and used to evaluate the exploration potential of shale gas in this area.

The regular test for the shale gas concentration includes three parts, namely free gas, adsorbed gas and dissolved gas, respectively. In this study, the adsorbed gas was only tested similar as the coal bed methane. The field desorption experiment was run to test the lost and adsorbed gas exclude the dissolved gas. The lost gas is adsorbed from rock during the lifting period from the well bottom to surface. With the USBM method of the USGS, the lost gas amount is proportional to the square root of desorption time, and restored according to the 4 hours' data before the desorption process. The sample was canned, and the desorbed gas was measured with the burette, including two parts of the desorbed gas obtained during the core canned and the residual gas released during the sample crushing course.

4. Source Rock

4.1 Sedimentary characteristics:

The potential source rocks are primarily concentrated in the favorite facies of the Taiyuan and Shanxi formations, which are shore swamp, floodplain marsh of delta plain, and river channel microfacies. They are gray and dark gray mudstone and coal bearing strata. The Taiyuan formation is 90-180 m and thicker in the Tianhuan sag and Yishan slope and divided into two sections (Figure 2). The sections primarily consist of mudstone, sandstone and multiple-layer coal beds. For example, the formation in the X2 well is mainly grey or black mudstone (Figure 3A), battie (Figure 3B), gray green sandstone, and glutenite sandwiched with multiple layers of coal (Figure 3C). The dark mudstone has abundant organic matters (Figure 3D) with 5-25m single thickness and 50m cumulative thickness, about accounted for 40% of the total formation thickness.

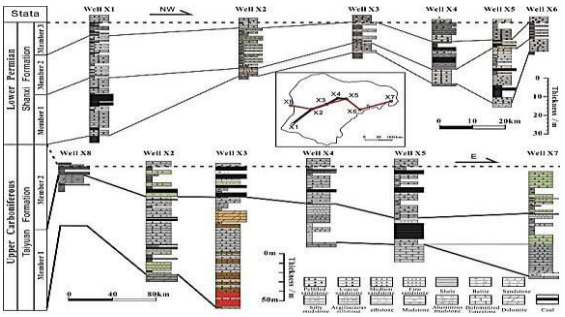

Figure2*. Well Profile between Taiyuan formation and Shanxi formation*

The lithologic columns were built with the cuttings of eight drilling wells. In addition, the upper profile was marked with a blue line in the location map, while the lower one was marked with a red line.

Based on the regional stratigraphy, the Shanxi formation is 20-80 m thick with obviously thinner in the Tianhuan sag and Yishan slope, and mainly divided into three sections. The dark shale are well developed and mainly distributed in the second and third sections. Also taking X2 as an example, the formation consists of gray green silty mudstone, black shale, gray sandstone, glutenite, and coal (Figure 3E). The dark mudstones have the 5-18m single thickness and 28m cumulative thickness, about accounted for 60% of the total formation thickness. The siltstone or

sandstone sandwiched with the mudstone (Figure 3F) is favorite reservoir space for shale gas.

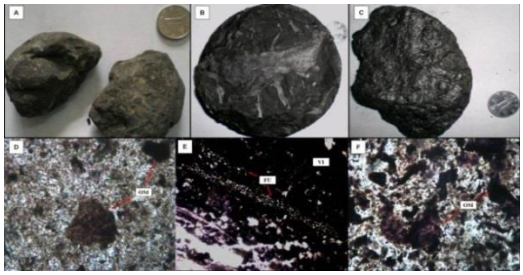

Figure3. *Feature of lithologic between Taiyuan formation and Shanxi formation*

A-grey mudstone, C_2t; B-battie, C_2t; C-coal, C_2t; D-shale, organic matter contained, C_2t, 40X; E-shale, organic matter contained, P_1s, 25X; F-coal, the fusinite and vitrinite can be distinguished, P_1s, 40X; OM-organic matter; FU-fusinite; VI-vitrinite

4.2 Geochemical Characteristics:

4.2.1 Content and type of organic carbon:

In the study area, the shale of two formations has higher organic carbon content (Figure 4). The Taiyuan formation has the higher organic carbon content in the Yishan slope, which primarily ranges from 1.08% to 4.20%; while the TOC of Shanxi formation is lower about 0.90% ~ 3.60%, and reaches the higher value at the two places of Yishan slope and Tianhuan sag.

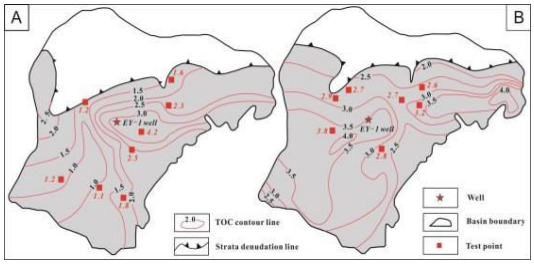

Figure4. *Contour of TOC in shale of Shanxi formation and Taiyuan formation*

A-Shanxi formation; B-Taiyuan formation

With the microscope, the organic carbon of Taiyuan mudstone mainly is humic including the Ⅲ, $Ⅱ_1$, and $Ⅱ_2$ types. The Shanxi organic carbon consists of Ⅲ and $Ⅱ_2$ types with a few Ⅰ and $Ⅱ_1$ types.

4.2.2 Organic carbon maturity:

Today, the Taiyuan shale has a high maturity, and R_o% ranges from 0.7% to 2.1% (Figure 5). The center and west of Central uplift have the higher maturity, and generally reach the high maturation ever overmature stage. The R_o% benefits organic matter to generate the gas for the thermolysis. Meanwhile, the R_o% of Shanxi shale ranges from 0.71% to 1.99%, a litter lower than Taiyuan formation, and have the max value near the east of Tianhuan sag. The maturation degree is similar to that in the Taiyuan formation.

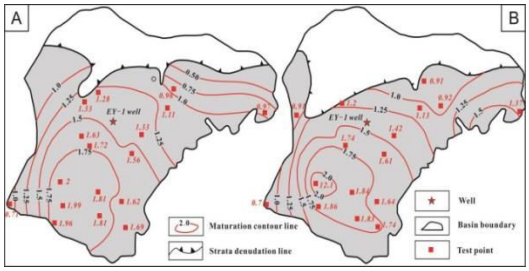

Figure5. *Contour of maturation in shale of Shanxi formation and Taiyuan formation A-Taiyuan formation; B-Shanxi formation*

5. Reservoir

5.1 Mineral characteristic:

With the whole rock mineral analysis with of X-ray diffraction, the Taiyuan shale has 37.6% clay mineral, 54.1% quartz and feldspar, and 8.3% carbonate mineral (Figure 6). However, the Shanxi shale consists of 57.5% clay mineral, 39.5% quartz and feldspar, and 3% carbonate mineral. Hence on average, the shale of the two formations has more clay mineral about 52.3%, 41.2% quartz and feldspar, and 3% carbonate mineral. The Shanxi shale has more clay content, indicating the micro pores are well developed. The Taiyuan shale has more quartz and feldspar, which can develop more brittle cracks. The carbonate mineral is less in this two formation, showing the shale can't be easily eroded and develop fewer pore and vug in the following diagenetic stage.

The Shanxi clay mineral has 44.9% illite, 33.6% kaolinite, 10% andreattite, and 11.5% chlorite. The Taiyuan clay mineral has 25.5% illite, 57.1% kaolinite, 8.5% andreattite, and 8.9% chlorite. The Taiyuan formation has less kaolinite and more illite than Shanxi formation. The clay minerals in the two formations are primarily composed of the kaolinite and illite. However, the lower content of smectite benefits for the reservoir fracturing.

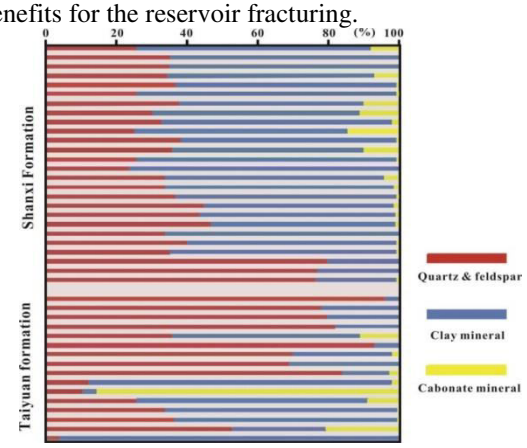

Figure6. *Content of mineral in shale of Shanxi formation and Taiyuan formation*

5.2 Porosity and permeability:

The reservoir space includes the matrix pores and fractures. The matrix pore is the residual primary one distributed between the silty grains, which decreases

quickly with the increasing burial depth. The micro pore can be developed during the organic matter generating hydrocarbon, which is chief type in the shale. Based on the research [3, 24], the shale with 7% TOC can create 4.9% porosity during its 35% organ matter generating hydrocarbon, indicating the creating pore greatly contribute for the reservoir quality. Under the electron mirror, the micro pores, created by the organ matter generating hydrocarbon, are generally several hundred nanometers in diameter (Figure 7). In addition, the micro pores are also created during the diagenetic changes, such as the clay mineral utilization, nonresistance mineral (feldspar and calcite) corrosion.

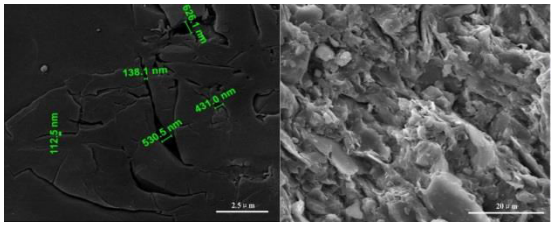

Figure7. *Micro pores of the shale under the electron mirror, (Left) backscattered electron image of the micro pores created by the organ matter generating hydrocarbon, C_2t; Right-scanning electron micrograph of the micro pores created during the clay mineral diagenetic changes, C_2t.*

With the nuclear magnetic logging and core mercury intrusion methods, the porosity and permeability of the two formations were analyzed in the EY-1 well. In the well, 46.76m Shanxi formation and 96.79m Taiyuan formation were drilled. From the T2 relaxation spectrum, the reservoir space is primarily composed of the medium-small and large-medium pores. The reservoir has the porosity less than 12% and permeability less than $12\times10^{-3}\mu m^2$, and can be divided into three types from the differential and shifted spectrums (Figure 8). The first type reservoir has lower GR and consists of two group pores, which are large-medium and shall, indicating that it could be sandstone and silty sandstone. The active porosity and permeability tested by NMR logging have two peaks in Shanxi formation and three peaks in the Taiyuan formation (Figure 9). The reservoir sections have obvious gas shows in the differential spectrum (TWS-TWL), and the TEL spectrum peak is obvious shifted forward, indicating that they are gas-bearing sections by the logging interpretation. The second type reservoir has higher GR, lower active porosity, and lower permeability, which is the mudstone. The reservoir sections have fewer gas shows in TWS-TWL, and the TEL spectrum peak is indistinct shifted forward. The third type reservoir has vague T2 spectrum, higher GR value, lower porosity and lower permeability, which is the coal bed. From the differential and shifted spectrums, the reservoir fluid shows can't be seen obviously.

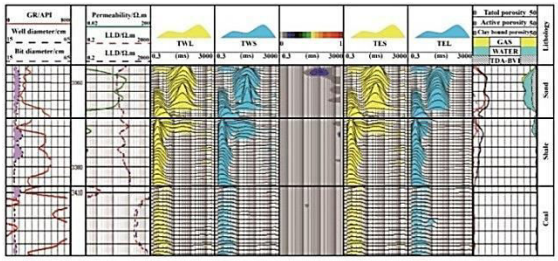

Figure8. *The response characteristics of magnetic resonance imaging log for shale of Shanxi and Taiyuan formations*

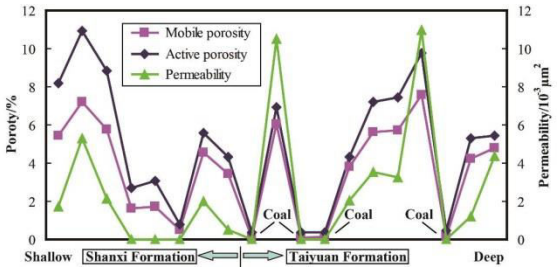

Figure 9*. Feature of porosity and permeability in shale between Shanxi formation and Taiyuan formation*

The relationship between the TOC and porosity measured by the mercury intrusion is not well correlated (Table 1). The reservoir has high TOC content, but the porosity is uncertain. In addition, the deep buried shale with a high maturation has an indeterminate porosity than the shallow buried one, indicating that the porosity increased a little during the hydrocarbon generation. In brief, the reservoir porosity is decided by the development degree of pores and fractures.

Table1*. Relationship between TOC and porosity of shale in Shanxi formation and Taiyuan formation*

Depth/m	Fm.	Lithology	TOC/%	Mercury intrusion porosity/%
3343	P_1s	mudstone	1.66	1.507
3353	P_1s	mudstone	0.11	1.388
3363	P_1s	mudstone	0.21	1.202
3369	P_1s	fine sandstone intercalated with mud	1.10	1.075
3378	P_1s	mudstone	0.74	0.952
3383	P_1s	fine sandstone intercalated with mud	0.10	0.532
3390	C_2t	mudstone	2.08	0.514
3411	C_2t	mudstone	0.47	0.157
3420	C_2t	carbonaceous	1.97	0.450
3426	C_2t	mudstone	0.90	0.500
3460	C_2t	carbonaceous shale	7.33	0.921
3463	C_2t	carbonaceous shale	4.30	0.693
3473	C_2t	mudstone	1.45	0.454

5.3 Pores and fractures:

In the imaging logging, the pitting holes can be seen in the sandstone sections (Figure 10A and 10B), which are dark colors, differently sized, and randomly distributed. The presence of holes will increase the reservoir porosity and permeability. According to the fracture statistics in the core imaging logging, the Shanxi formation develops two open fractures, one high resistive fracture, and eight semi-filled fractures mainly developed in the sandstone sections. In Taiyuan formation, the fractures mainly developed with a low angle of less than 60º, including 19 semi filled fractures and 17 open fractures (Figure. 10C). The striking directions of the fractures are mainly NE-SW, which are consistent with the nearby faults and situ stress direction. The holes connected by the fractures greatly increase the reservoir infiltrating capacity [25].

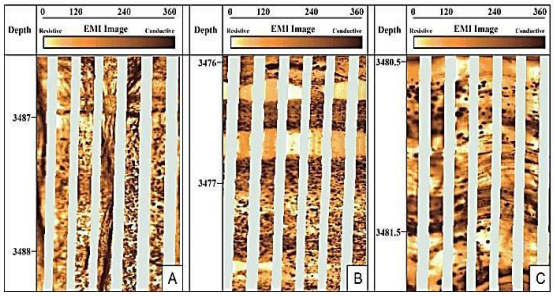

Figure10. *The fractural and vuggy response characteristics of micro-resistivity imaging log for shale of Shanxi and Taiyuan formations* A-the pitting holes are obviously identified, and an induced fracture is recognized; B- the pitting holes are obviously identified; C-five dark sine curves are recognized as the open fractures

6. Gas Bearing Analysis:

The Shanxi mudstone including the siltstone has the desorbed gas content of 0.173 ~ 0.465m^3/t (average 0.328 m^3/t) and the lost gas content of 0.830 ~ 6.800 m^3/t (average 2.915 m^3/t), and the total gas content is 0.220 ~ 6.973 m^3/t (average 3.243 m^3/t); The Shanxi sandstone has the desorbed gas content of 0.133 ~ 0.338 m^3/t (average 0.253 m^3/t) and the lost gas content of 0.950 ~ 12.080 m^3/t (average 3.900 m^3/t), and total gas content is 1.113 ~ 12.372 m^3/t (average 4.153 m^3/t). The Taiyuan mudstone and siltstone have the desorbed gas content of 0.229 ~ 3.368m^3/t (average 0.784 m^3/t) and the lost gas content of 1.000 ~ 4.560 m^3/t (average 2.613 m^3/t), and the total gas content is 1.229 ~ 5.668 m^3/t (average 3.397 m^3/t); The Taiyuan sandstone has the desorbed gas content of 0.298 ~ 0.633 m^3/t (average 0.431 m^3/t) and lost gas content of 3.860 ~ 6.700 m^3/t (average 5.200 m^3/t), and the total gas content is 4.362 ~ 7.333 m^3/t (average 5.631 m^3/t); The Taiyuan coal has the desorbed gas content of 8.053 ~ 14.065 m^3/t (average 11.566 m^3/t) and the lost gas content of 7.420 ~ 12.103 m^3/t (average 10.828 m^3/t), and the total gas content is 19.536 ~ 26.065 m^3/t (average 22.394 m^3/t). The Taiyuan formation has higher gas content than Shanxi formation, whether the shale or the sandstone, especially higher gas content in the coal (Figure 11). The shale gas content of the five sets in the United States ranges from 0.42 to 9.91 m^3/t, mostly less than 3m^3/t [26-27]. In contrast, the two formations also have a large exploration and development potential in this study, especially CBM in the coal beds.

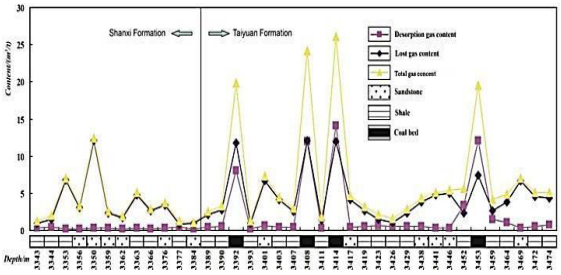

Figure11. *Feature of Gas-bearing in Shanxi and Taiyuan formations*

7. Conclusions

(1) The Shanxi and Taiyuan formations develop high quality shale, which is thick and distributed in the two sections of Taiyuan formation and the upper two sections of Shanxi formation. The shale has high organic matter content, and the organic matter is humic at the maturity stage even over-mature stage, which benefits for generating gas.

(2) The Taiyuan mudstone is brittle with more quartz, while the Shanxi mudstone has more clay content with micro pores. The clay mineral of two formations primarily consists of the kaolinite and illite. The siltstone or sandstone sandwiched with the mudstone is favorite reservoir space for shale gas. The shale reservoir space includes the matrix pores and fractures, which is decided by the development degree of pores and fractures.

(3) Whether the shale or sandstone in the Taiyuan formation, has higher gas content than Shanxi formation, especially higher gas content in the coal. The two formations have a large exploration and development potential compared with the American shale gas.

8. Acknowledgements

This work was supported by the Key Scientific and Technological Projects of Shanxi Province (MQ2014-02) and National Natural Science Foundation of China (No. 41272155).

References

[1] Bowker, K.A., "Barnett Shale gas production, Fort Worth Basin: Issues and discussion". *AAPG Bulletin,* Vol. 91, No. 4, (2007), 523–533.

[2] Hill, D.G., and Nelson, C.R., "Reservoir properties of the Upper Cretaceous Lewis Shale, a new natural gas play in the SanJuan Basin", *AAPG Bulletin,* Vol. 84, No. 8, (2000), 12-40.

[3] Jarvie, D.M., Hill, R.J., Ruble, T.E., and Pollastro, R.M., "Unconventional shale-gas systems: The Mississippian Barnett Shale of north-central Texas as one model for thermogenic shale-gas assessment". *AAPG Bulletin,* Vol. 91, No. 4, (2007), 475-499.

[4] Ross, D.J.K., and Bustin, R.M., "Shale Gas Potential of the Lower Jurassic Gordondale Member, Northeastern British Columbia, Canada", *Bulletin of Canadian Petroleum Geology,* Vol. 55, No. 1, (2007), 51-75.

[5] Javadpour, F, Fisher, D, and Unsworth, M., Nanoscale Gas Flow in Shale Gas Sediments. *Journal of Canadian Petroleum Technology,* Vol. 46, No. 10, (2007), 55-61.

[6] Loucks, R.G., Reed, R.M., Ruppel, S.C., and Jarvie, D.M., "Morphology, Genesis and Distribution of Nanometer-Scale Pores in Siliceous Mudstones of the Mississippian Barnett Shale", *Journal of Sedimentary Research,* Vol. 79, No. 12, (2009), 848-861.

[7] Sachsenhofer, R.F., Bechtel, A., Kuffner, T., Rainer, T., Gratzer, R., Sauer, R., and Sperl, H., "Depositional environment and source potential of Jurassic coal-bearing sediments (Gresten Formation, Höflein gas/condensate field, Austria)", *Petroleum Geoscience,* Vol. 12, (2006), 99-114.

[8] Schulz, H.M., Biermann, S., Berk, W.V., Krüger, M., Straaten, N., Bechtel, A., Wirth, R., Lüders, V., Schovsbo, N.H., and Crabtree, S, "From shale oil to biogenic shale gas: Retracing organic-inorganic interactions in the Alum Shale (Furongian-Lower Ordovician) in southern Sweden", *AAPG Bulletin,* Vol.99, No. 5, (2015), 927-956.

[9] Skompski, S., Luczynski, P., Drygant, D., and Kozlowski, W., "High-energy sedimentary events in lagoonal successions of the Upper Silurian of Podolia, Ukraine. Facies 54: 277-296. Lanés S (2005). Late Jurassic to early Jurassic sedimentation in northern Neuquén Basin, Argentina. Tectosedimentary evolution of the first trangression", *Geologica Acta,* Vol. 3, No. 3, (2008), 81-106.

[10] Chen, S.B., Zhu, Y.M., Wang, H.Y., Liu, H.L., Wei, W., Luo, Y., Li, W., and Fang, J.H., Research status and trends of shale gas in China. *Acta Petrolei Sinica,* Vol. 31, No. 4, (2010), 689-694.

[11] Dong, D.Z., Cheng, K.M., Wang, S.Q., and Lu, Z.G., "An evaluation method of shale gas resource and its application in the Sichuan basin", *Natural Gas Industry,* Vol. 29, No. 5, (2009), 33-39.

[12] Li, C.W., Tao, S.Z., Dong, D.Z., and Guan, Q.Z., "Comparison of the formation condition of shale gas between domestic and abroad and favorable areas evaluation", *Natural Gas Geoscience,* Vol. 26, No. 5, (2015), 986-1000.

[13] Zou, C.N., Dong, D.Z., Yang, H., Wang, Y.M., Huang, J.L., Wang, S.F., and Fu, C.X., "Conditions of shale gas accumulation and exploration practices in China", *Natural Gas Industry,* Vol. 31, No. 12, (2011), 26-39.

[14] Zhang, J.C., Xu, B., Nie, H.K., Wang, Z.Y., and Lin, T., "Exploration potential of shale gas resources in China", *Natural Gas Industry,* Vol. 28, No. 6, (2008), 136-140.

[15] Zhao, W.Z., Dong, D.Z., Li, J.Z., and Zhang, G.S., "The resource potential and future status in natural gas development of shale gas in China", Engineering Sciences, Vol. 14, No. 7, (2012), 46-52.

[16] Zhang, J.C., Jiang, S.L., Tang, X., Zhang, P.X., Tang, Y., and Jin, T.Y., "Accumulation types and resources characteristics of shale gas in China", *Natural Gas Industry,* Vol. 29, No. 12, (2009), 109-114.

[17] Wang, X.Z., Gao, S.L., and Gao, C., "Geological features of Mesozoic continental shale gas in south of Ordos Basin, NW China", *Petroleum Exploration and Development,* Vol. 41, No. 3, 41(3), (2014), 294-304.

[18] Zou, C.N., Yang, Z., Tao, S.Z., Li, W., Wu, S.T., Hou, L.H., Zhu, R.K., Yuan, X.J., Wang, L., Gao, X.H., Jia, J.H., Guo, Q.L., and Bai, B., "Nano-hydrocarbon and the accumulation in coexisting source and reservoir", *Petroleum Exploration and Development,* Vol. 39, No. 1, (2012), 13-26.

[19] Wang, S.J., Li, D.H., Li, J.Z., Dong, D.Z., Guang, W.Z., and Ma, J., "Exploration potential of shale gas in the Ordos Basin", *Natural Gas Industry,* Vol. 31, No. 12, (2011), 40-46.

[20] Chen, R.Y., Luo, X.R., Zhao, W.Z., and Wang, H.J., "Thermal anomaly and thermal evolution of source rocks in Mesozoic, Ordos Basin", *Petroleum Exploration and Development,* Vol. 34, No. 6, (2007), 658-663.

[21] Wang, C.G., Wang, Y., Xu, H.Z., Sun, Y.P., Yang, W.L., and Wu, T.H., "Discussion on evolution of source rocks in Lower Paleozoic of Ordos Basin", *Acta Petrolei Sinica,* Vol. 30, No. 1, (2009), 38-45.

[22] Ahmed Mahmoudi, Imen Mejri, "Analysis of conduction-radiation heat transfer with variable thermal conductivity and variable refractive index: application of the lattice boltzmann method", *International Journal of Heat and Technology,* Vol. 33, No. 1, (2015), 1-8.

[23] N. Nithyadevi, A. Shamadhani Begum, and C. Udhaya Shankar, "Buoyancy and thermocapillary driven flows in an open cavity with bottom heating and symmetrical cooling from sides", *International Journal of Heat and Technology,* Vol. 33, No. 1, (2015), 63-70.

[24] Cao, Y.H., Cui, X.M., "Natural convection of power law fluids in porous media with variable thermal and mass diffusivity", *International*

Journal of Heat and Technology, Vol. 33, No. 2, (2015), 85-90.

[25] Feng Fuping, Ai Chi, Xu Haisu, Cui Zhihua, and Gao Changlong, "Research on the condition model of drilling fluid nonretention in eccentric annulus", *International Journal of Heat and technology,* Vol. 33, No. 1, (2015), 9-16.

[26] Tang, Y., Li, L.Z., and Jiang, S.X., "A logging interpretation methodology of gas content in shale reservoirs and its application", *Natural Gas Industry,* Vol. 34, No. 12, (2014), 46-54.

[27] Yao, S.G., Jia, X.W., Huang, T., and Duan, L.B., "Numerical simulation of bubble motion in boiling nanofluids based on lattice boltzmann method", *International Journal of Heat and Technology*, Vol. 33, No. 1, (2015), 71-76.